International Journal of Science and Research Archive
eISSN: 2582-8185
Cross Ref DOI: 10.30574/ijsra
Journal homepage: https://ijsra.net/



(RESEARCH ARTICLE)

Check for updates

GEOSPATIAL DISTRIBUTION AND MAPPING OF HYDROCARBON-CONTAMINATED SITES IN SELECTED COMMUNITIES OF THE NIGER DELTA, NIGERIA

Onisosweiya Emem [1, 3, *], T.K.S. Abam [1, 2] and H.O. Nwankwoala [1]

[1] Department of Geology, Rivers State University, Port Harcourt, Nigeria.
[2] Institute of Geosciences and Environmental Management, Rivers State University, Port Harcourt Nigeria.
[3] Centre of Excellence for Environmental Restoration, Federal Ministry of Environment, Nigeria.
* Corresponding Author

ORCID Details
Onisosweiya Emem: https://orcid.org/0009-0004-8523-3977
Tamunoene Kingdom Simeon Abam: https://orcid.org/0000-0003-3226-4855
Hycienth Ogunka Nwankwoala: https://orcid.org/0000-0002-7049-9658

International Journal of Science and Research Archive, 2026, 21(02), 022–036

Publication history: Received on 16 September 2026; revised on 28 October 2026; accepted on 30 October 2026

Article DOI: https://doi.org/10.30574/ijsra.2026.21.2.1944

Copyright © 2026 Author(s) retain the copyright of this article. This article is published under the terms of the Creative Commons Attribution License 4.0

ABSTRACT

Hydrocarbon contamination from anthropogenic activities remains a major environmental challenge in the Niger Delta. Accurate geospatial mapping of contaminant plumes is required for targeted remediation. To assess the geospatial distribution and lateral extent of hydrocarbon-impacted soils in two selected communities. Auger hole sampling was conducted at seven locations (AH1-AH7) plus a control (C) in Ajeokpori (Study Area 1) and Aabue-Korokoro Well 003 (Study Area 2). Coordinates were acquired with GPS in a projected metric system. Hydrocarbon impact was classified empirically as Low (<1000 mg/kg TPH), Medium (1000-5000 mg/kg TPH) and High (>5000 mg/kg TPH) in line with EGASPIN. Plume lateral extent was interpreted from Electrical Resistivity Tomography (ERT) profiles. In Study Area 1 (Ajeokpori), plume extents ranged from 68 m to 157 m. Five locations (AH1, AH2, AH3, AH4, AH6) were medium-impact (150-157 m) while two (AH5 - 68 m, AH7 - 144 m) were high-impact. AH5 and AH7 cluster within ~111 m along a N-S alignment south of AH1-AH4. In Study Area 2 (Aabue-Korokoro), extents ranged from 35 m to 135 m (mean 96.4 m). Four locations (AH1-AH4) were low-impact, two (AH5-115 m, AH6-105 m) medium-impact, and one (AH7-80 m) high-impact. Medium-impact points AH5 and AH6 form a 12.2 m cluster in the southwest, while AH7 represents the southernmost hotspot. The study demonstrates that lateral extent does not equate to impact severity. Contamination is spatially heterogeneous. High-impact hotspots require targeted remediation, while extensive low and medium-impact plumes require boundary delineation. The geospatial framework provides a basis for ERT verification and monitoring.

Keywords: Geospatial mapping, Hydrocarbon contamination, TPH, Plume extent, Niger Delta, ERT, GIS

1 INTRODUCTION

Geospatial Distribution of Hydrocarbon-Contaminated Sites has demonstrated as one of the most significant systems of environmental degradation in the Niger Delta region of Nigeria, mainly attributed to crude oil exploration, production, transportation, pipeline vandalism, and artisanal refining activities. [1,2]. Satellite imagery has proven effective for mapping anthropogenic activities and land surface dynamics [3]. The region has experienced more than 16,0000 spill incidents between 2006 and 2023, resulting in the release of more than 800,000 barrels of crude oil into the environment [4]. This has resulted in widespread contamination of soils, surface water, groundwater, and sediments, posing serious threats to ecosystem health, food security, and human well-being.

Hydrocarbon-contaminated sites refer to locations where concentrations of Total Petroleum Hydrocarbons (TPH), Polycyclic Aromatic Hydrocarbons (PAHs), and Benzene, Toluene, Ethylbenzene and Xylene (BTEX) exceed regulatory limits prescribed by the Department of Petroleum Resources (DPR) and the Environmental Guidelines and Standards for the Petroleum Industry in Nigeria (EGASPIN). According to the United Nations Environment Programme [1] assessment of Ogoniland, hydrocarbon contamination was found to penetrate up to 5 meters deep in more than 49 sites, with contamination exceeding Nigerian national standards at two-thirds of sites assessed near oil facilities [1].

Geospatial distribution of Hydrocarbon-Contaminated Sites is the spatial arrangement and pattern of hydrocarbon impact across a geographic area, analyzed using Geographic Information Systems (GIS), remote sensing, and Global Positioning Systems (GPS). Geospatial analysis provides critical insights into the clustering, density, and dispersion patterns of pollution [5]. Recent studies have demonstrated that oil spill distribution in the Niger Delta follows a clustered pattern, with significant hotspots [6,3]. Techniques such as Kernel Density Estimation, Hexbin mapping, Contour mapping, and Inverse Distance Weighting (IDW) interpolation have been effectively used to delineate pollution hotspots and regional variation in TPH concentrations [7]. Studies in Oyigbo, Rivers State, showed that approximately 46% of sampled locations exceeded the World Health Organization [8] acceptable limit of 50 mg/L for TPH, with higher pollution dispersion in Northern and North-western axes [5].

Persistent soil and groundwater contamination has been observed in communities such as Ajeokpori and Aabue-Korokoro, largely due to their coarse-textured sandy loam soils with high permeability. These communities are characterized by legacy oil and gas infrastructure left unattended.

Despite several cleanup exercises initiated by the Hydrocarbon Pollution Remediation Project (HYPREP), and Shell Petroleum Development Company (Renaissance), Ogoniland still lacks systematic, large-scale, site-specific geospatial information on contamination hotspots, particularly at community level. Therefore, mapping the geospatial distribution of hydrocarbon-contaminated sites in communities is critical for understanding the spatial extent, identifying exposure pathways, and prioritizing remediation efforts.

2 STUDY AREA

The project sites are Ajeokpori, study area 1 [Eastings (WGS 84, Zone 32N):294542 / Northings (WGS 84, Zone 32N):532224], Ogale community, Eleme Local Government Area and Aabue-Korokoro community, study area 2 [Eastings (WGS 84, Zone 32N):312829 / Northings (WGS 84, Zone 32N): 524315], both in Tai Local Government Area of Rivers State. The area of study area 1 is 34,600 square meters and the area of study area 2 is 24,922.2 square meters. The distance between the two study areas is 20,027.01m (see figure 1).



Figure 1: Google imagery showing distance between Ajeokpori, Ogale and Aabue-Korokoro (Well 003) in Eleme and Tai LGAs, Rivers State. Nigeria

The spill in Ajeopkori, (study area 1) was located next to an oil pipeline while the spill in Aabue-Korokoro (study area 2) was near the Renaissance African Energy Company (former Shell Petroleum Development Company-SPDC) Well 003 crude oil facility. The study areas are situated within the low-lying sedimentary terrain of the Niger Delta, underlain by the unconsolidated coastal plain sands of the Benin Formation, characterized by high permeability which enhances contaminant migration. The topography of both places is mostly flat and between 19m and 20m above sea level.



Figure 2: Google imagery showing 2-D ERT orientation of the survey lines across the study area 1 (Ajeokpori, Ogale).

The red line area (see Fig. 1) is the possible hydrocarbon impacted delineated area identified in the UNEP 2011 report, whereas the yellow line is oil pipeline right of way.

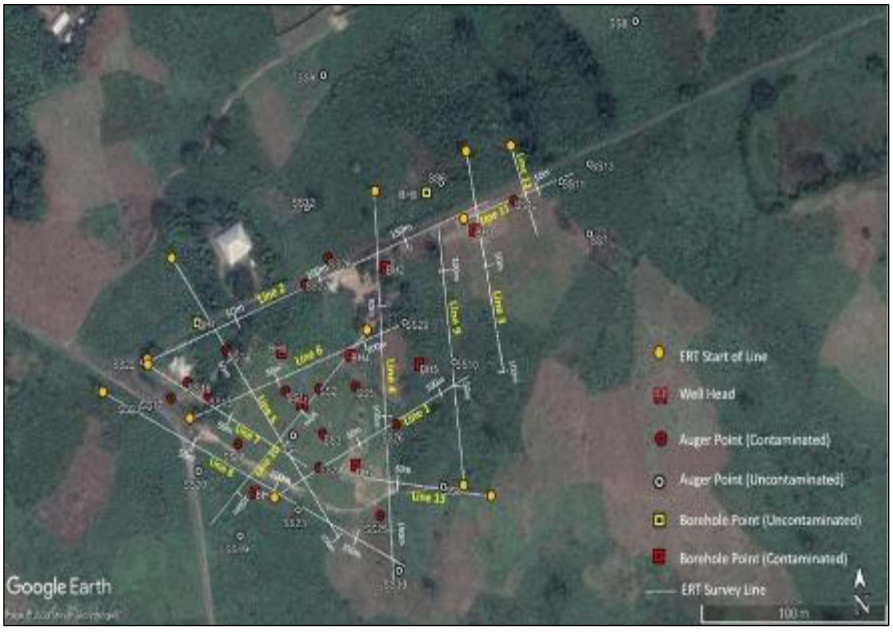


Figure 3: Google imagery showing 2-D ERT orientation of the survey lines across the Well Head (Well 003), Aabue- Korokoro area (study area 2).

2.1 Climate and Geohydrology

The study location is characterized by a tropical climate with high temperatures and high levels of rainfall throughout the year [9], influenced by its proximity to the Atlantic Ocean and the dominance of maritime air masses. The region experiences a humid tropical climate, with mean annual rainfall ranging from 2,500 mm to 4,000 mm [10]. The rainy season typically lasts from March to October, with the heaviest rainfall occurring between June and September [11]. The wet season typically extends from March to October, with peak rainfall occurring between June and September, whereas the dry season, generally lasts from November to February. This pattern, which seem predictable has now become dynamic as a possible result of climate impact. The high rainfall intensity is responsible for extensive surface runoff, flooding, and the development of numerous creeks, rivers, and wetlands throughout the region [12]. Regional (Niger Delta) mean annual temperatures ranges from 26°C to 32°C. Relative humidity is also consistently high, often exceeding 80%, particularly during the rainy season. The combination of high rainfall, temperature, and humidity contributes to intense chemical weathering and groundwater recharge processes within the region [13]. The study location is a low-lying coastal plain, with an elevation ranging from 2-7 meters above sea level.

The geohydrology of the Niger Delta is closely linked to its sedimentary geology and depositional history, which were formed during the Tertiary period through the accumulation of fluvial and marine sediments transported by the Niger River. The subsurface stratigraphy of the region is commonly divided into three major lithostratigraphic units: the Benin Formation, Agbada Formation, and Akata Formation [14]. The groundwater table ranges from 1.35m to 38m. Groundwater within this formation typically occurs under unconfined to semi-confined conditions, making it easily accessible through shallow boreholes and wells [12].

Groundwater recharge in the Niger Delta primarily occurs through direct infiltration of rainfall, facilitated by the region's high precipitation and permeable sandy soils. The shallow water table, which commonly occurs within 1–10 m below ground level, contributes to the formation of extensive wetlands, swamps, and mangrove ecosystems [12].

Surface water systems in the Niger Delta are dominated by a complex network of rivers, creeks, estuaries, and tidal channels, which are strongly influenced by tidal fluctuations from the Atlantic Ocean. This interaction between surface water and groundwater often results in salinity intrusion in coastal aquifers, particularly in areas close to tidal creeks and estuaries [13].

The geohydrological characteristics of the Niger Delta, including its high permeability sediments, shallow groundwater table, and extensive surface water networks, make the region particularly vulnerable to groundwater contamination, especially from hydrocarbon spills and other anthropogenic activities associated with oil exploration and production [12].

Surface water systems in the Niger Delta are dominated by a complex network of rivers, creeks, estuaries, and tidal channels, which are strongly influenced by tidal fluctuations from the Atlantic Ocean. This interaction between surface water and groundwater often results in salinity intrusion in coastal aquifers, particularly in areas close to tidal creeks and estuaries [13].

The geohydrological characteristics of the Niger Delta, including its high permeability sediments, shallow groundwater table, and extensive surface water networks, make the region particularly vulnerable to groundwater contamination, especially from hydrocarbon spills and other anthropogenic activities associated with oil exploration and production [12].

2.2 Geologic and Tectonic Settings

The geology of the study area is predominantly characterized by Quaternary sediments, consisting mainly of unconsolidated deposits. The dominant lithological units within the upper subsurface include clay, clayey sand, clayey silt, sandy clay, sandy silt, silt clay, and silty sand, extending to an approximate depth of 7 m below ground level. These sediments reflect the heterogeneous depositional environment typical of recent alluvial and deltaic settings. The Akata Formation serves as the principal source rock for hydrocarbons in the Niger Delta basin due to the presence of organic-rich marine sediments that have undergone thermal maturation at depth (Reijers, 2011).

Structurally, the Niger Delta is characterized by a complex system of growth faults, rollover anticlines, and shale diapirs, which developed as a result of gravitational instability within the thick sedimentary sequence. These structures play a crucial role in the migration and accumulation of hydrocarbons, creating numerous oil and gas traps within the basin (Doust & Omatsola, 1990).

Sedimentation within the Niger Delta continues today, with large volumes of sediments transported annually by the Niger River and deposited across the delta plain and continental shelf. The modern delta environment consists of a network of distributary channels, tidal flats, mangrove swamps, freshwater swamps, and barrier island systems, reflecting the dynamic interaction between fluvial, marine, and tidal processes [15].

Overall, the geological setting of the Niger Delta reflects a complex interplay of tectonic activity, sediment supply, and marine processes, which have collectively contributed to the formation of one of the most prolific hydrocarbon provinces in the world.

3 STUDY MATERIALS AND METHODS

The data of the results of this study were directly obtained in the field, reviewed, discussed and drew conclusion.

The study was conducted to determine how well hydrocarbon contaminants in the subsurface environment are mapped and geospatially distributed, in the study locations, considering volume of spill, where they occur and migration direction (pathways).

3.1 Materials used for the study

The materials utilized for the study included four terrameters (ABEM SAS 1000, ABEM SAS 300, Rhomega-Smart and AQMC Soil Resistivity Meter), 156 multi-electrodes, 19 reels of cable, 10 measuring tapes, 4 Garmin Global Positioning Systems (GPS), 4 twelve-volt batteries, 16 hammers, base maps of the study area, data recording sheets, and a digital georeferencing camera. Materials used in soil sampling of hydrocarbon contaminated site include stainless-steel hand augers, core samplers, trowels, scoops, and spatulas for collecting soil at selected depths; laboratory-supplied glass jars with suitable lined caps for petroleum analyses and dedicated sealed sampling devices, prepared vials for volatile compounds such as TPH, PAHs, BTEX ; measuring tapes, and marker pegs for locating sampling points; and labels, field notebooks, and chain-of-custody forms for documentation. Coolers with ice packs for preservation during transportation, while nitrile gloves, safety boots, coveralls, and protective eyewear protect personnel. Detergent, clean water, laboratory-grade rinse water, and brushes for decontamination of reusable equipment and prevention of cross-contamination.

3.2 Methods used for the study

The intention was to perform both 2D and 3D ERT surveys. The 3-D ERT surveys were necessary to assess the extent of the contaminated soil and the area it covered. The survey method was the Wenner array configuration. The Wenner 2-D array was selected for its sensitivity to the depth, width and trajectory of the plumes as they flow. In this method the lateral extent of the investigation is determined by the electrode array spread, and the depth of investigation is determined by the electrode spacing. The depth of investigation increases with an increasing electrode spacing for a given array spread [17]. Figures 2 and 3 are Google images of the orientation of survey lines used in this study. Hydrocarbon impact was classified empirically based on TPH concentration in line with EGASPIN (2018) as Low (<1000 mg/kg), Medium (1000-5000 mg/kg) and High (>5000 mg/kg). The control point was established 100 meters from the site of the damage.

3.3 Technical Data

Data sheets were pre-designed for the survey to facilitate the recording of all the measurements taken. Along with these sheets came information regarding how to set up the survey, the precise measurements to be made, the distances between the existing and prospective electrodes, the geometric factors associated with those distances, and the resistance values in ohms.

3.4 Earth Imager RES2DINV and RES3DINV Software

The software used for processing and interpretation of two-dimensional (2D) and three-dimensional (3D) resistivity and induced polarisation (IP) data is the Electrical Resistivity Tomography (ERT) inversion software Earth Imager. The software, commonly used in environmental, engineering and groundwater investigations, uses smooth and strong inversion constraints to produce accurate subsurface resistivity models [18].

The processing and interpretation of the Electrical Resistivity Tomography (ERT) data can be carried out by the well-known inversion programs RES2DINV and RES3DINV. These software programs use least-squares optimisation methods to produce subsurface resistivity models from two-dimensional (2D) and three-dimensional (3D) data sets. They are good at computing. They can handle a wide variety of electrode arrays. They are used a lot in geotechnical, hydrogeological and environmental investigations [19]. The resistivity threshold of ≤600 Ωm was used as cut-off value for the study for finding out if there might be hydrocarbons in the study area.

3.5 ERT working Principle

To measure electrical resistivity fields, you need to know the electric potential (V). This is the amount of energy lost when a current moves away from its source and spreads out in a plane that is perfectly flat and infinitely long. The potential function V = V (x, y, z) is influenced by three spatial coordinates. This yields a three-dimensional image of the subsurface geological systems. The theoretical potential in complex two- or three-dimensional geological models is calculated by numerical solution of the governing equations by means of computer programs [20].

Resistivity surveys are based on Ohm's Law which describes how electricity flows through the earth. For this study, the Wenner array configuration was selected as it achieved the goals of the study. The current electrodes (C1 and C2) are pushed outward into the ground to inject current; the potential electrodes (P1 and P2) are pushed inward to measure the potential difference between the current electrodes (see Figure 4). The depth at which the resistivity was studied can be found by multiplying the measured resistance of the subsurface to current flow by the correct geometric factor.

3.6 Study areas (Ajeokpori and Aabue Korokoro, Well 003)

For the Ajeokpori site in study area 1, the minimum electrode spacing was set at 1.50m, as the preliminary vertical electrical sounding (VES) indicated very shallow depths to contamination (1.30m). The maximum electrode spread was set at 12.0m. During the first electrode spread the distances between the present and potential electrodes remain the same at 1.50m and the survey continues along the whole profile line. The electrode spread is doubled to investigate deeper targets, and the survey is repeated along the line, and repeated, and repeated until a 12m spread is reached. As presented in Table 1, the shape of each survey line is shown with its length and geographic coordinates. The same idea was applied at the Aabue_Korokoro site, but the electrode spread was between 5 and 25 m. The survey line crossed the entire profile line in the first electrode spread, and the distances between the current electrode and the potential electrode were constant at 5 meters. This was at the Abue_Korokoro site. The shape of each survey line is shown in Figure 2, together with its length and geographical coordinates.

A three-dimensional resistivity model was constructed from the two-dimensional apparent resistivity data for each site to ensure full coverage of the study areas and to increase the accuracy of interpretation. This method was found to provide the best results for the characterisation of the subsurface [21].

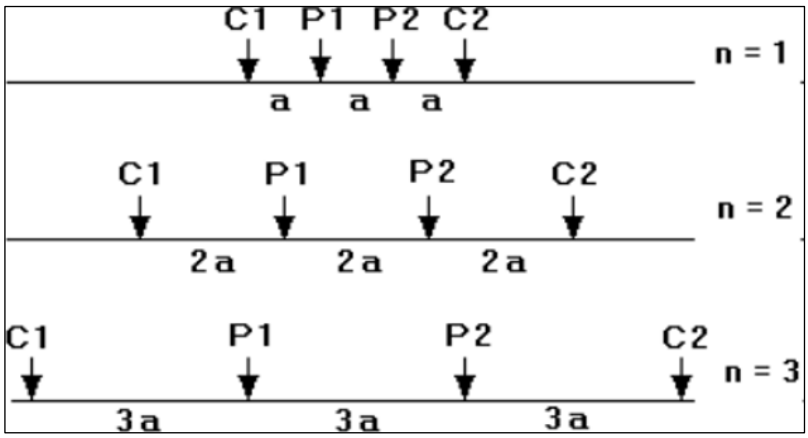


Figure 4: Wenner Array Configuration utilized for this study (Adapted from: Telford, et al. 1990)

Surveys can extend to depths of several hundreds of metres, beyond which data resolution progressively deteriorates, where choice of electrode array configuration may largely depend on the objectives of the survey [17].

3.7 Data Processing

The Earth Imager and RES2DINV inversion software was used for 2-D resistivity inversion. The software used for the 3D inversion was RES3DINV. The collected 2-D resistivity data was inverted by using the 2-D Earth Imager program and RES2DINV inversion software. The apparent resistivity values of each profile were compiled in a format that can be read by the Earth Imager inversion software and the RES2DINV software. In this study, the finite element method (FEM) was used for the 2-D modelling in Earth Imager. The finite difference and least-squares method were used for the 2-D modelling in RES2DINV and 3-D modelling of apparent resistivity data, respectively. The aim was to reconstruct the geological model that gives synthetic data matching the observed data set. The RES2DINV and RES3DINV programs automatically interchange between 2D and 3D views using the algorithm of [22]. The method is based on least-squares inversion with smoothness constraints [23] and is performed using a quasi-Newton optimisation technique [22].

The benefit of this approach is that the roughness and damping factors can be adjusted for different types of data [24]. Landforms along the survey line were not very interesting so no elevation data were used. During inversion, the finite-element method with four nodes per unit electrode spacing was used to obtain the apparent resistivity values.

The inversion process gave a good result after five tries with an RMS (root mean square) error of less than 10% for all the models that were made. So, the fifth attempt was supposed to give a geoelectrical image close enough to the true picture of resistivity distribution below the ground.

The subsurface is divided into several layers in the RES3DINV program, and each layer is divided into several rectangular cells [21]. The program tries to estimate the resistivity of the cells in the inversion model which is more similar to the measured values of apparent resistivity from the field survey. The resolution of the resistivity method rapidly decreases with depth. The division of the model cells into horizontal slices (called "depth slices") is only meaningful for the upper two layers. Not only were the model cells divided in the horizontal direction, but also in the vertical direction for accurate 3D imaging and interpretation.

4 DATA ANALYSIS

A total of 14 ERT lines (tables 1 – 2) were applied across the areas of study to establish hydrocarbon plum trajectory, pathway, depth and volume. Soil samples were collected and sent to laboratory Analysis of TPH, PAH, BTEX. The analyses were conducted following the best practices approved by APHA (American Public Health Association), and USEPA (United States Environmental Protection Agency); and as adopted by the Nigeria Upstream Petroleum Regulatory Commission (NUPRC), Nigeria Midstream and Downstream Petroleum Regulatory Authority (NMDPRA) and Federal Ministry of

Environment (FMEnv). A resistivity threshold of ≤600 Ω·m was adopted as the criterion for identifying hydrocarbon contamination in this study.

Table 1 ERT survey geometry, coordinates and interpreted outcomes at Ajeokpori (Study Area 1)

ERT Line No.	Length of Line (m)	Orientation of Line	Line Coordinates (E/N)		Outcome
Line 1	150	NE-SW	294642	531875	Large plume was observed across the entire line length.
Line 2	150	NW-SE	294412	532092	No hydrocarbon plume.
Line 3	157	NW-SE	294585	531968	Large plume of hydrocarbon observed across the entire line length.
Line 4	154	NE-SW	294591	531918	A large plume was observed across the entire line length.
Line 5	150	NW-SE	294506	532036	A single plume was observed with lateral spread
Line 6	150	NE-SW	294343.00	532141	No plume was observed across the total spread length.
Line 7	150	NW-SE	305313.00	519835	A large plume was observed with lateral and vertical spread.

Table 2 ERT survey geometry, coordinates and interpreted outcomes at Aabue-Korokoro Well 003 (Study area 2) site.

ERT Line No.	Length of Line(m)	Orientation of Line	Line Coordinates		Outcome
Line 1	115	NE-SW	312800 E	524266 N	Significant presence of hydrocarbon
Line 2	185	NE-SW	312732 E	524328 N	Contamination is evident from 50.0 m to the end of the survey line
Line 3	120	NNW-SSE	312910 E	524410 N	Contamination is evident from approximately 25.0 m to 35.0 m from the origin of the survey line
Line 4	175	N-S	312860 E	524397 N	Two distinct plumes are identified.
Line 5	145	NW-SE	312751 E	524371 N	A trending hydrocarbon lume with a _V‘ shape.
Line 6	120	NE-SW	312755 E	524302 N	Hydrocarbon plume extends from the origin to 105.0 m.
Line 7	100	NW-SE	312730 E	524326 N	Hydrocarbon plume exhibits three distinct occurrences.

Table 3. Georeferenced auger hole locations and hydrocarbon impact classification along the NNPC/NPSC pipeline at Ajeokpori (Study Area 1),

S/No	Plume Extent(m)	Coordinates		Label	Comment
		Easting	Northing		
1	150	294419	532023	AH1	Medium-impact
2	150	294461	532015	AH2	Medium-impact
3	157	294528	532063	AH3	Medium-impact
4	154	294598	532048	AH4	Medium-impact
5	68	294596	531967	AH5	High-impact
6	150	294489	531939	AH6	Medium-impact
7	144	294597	531856	AH7	High-impact
8	N/A	294413	532244	C	Control

Table 4 Georeferenced auger hole locations and hydrocarbon impact classification within Well 003, Aabue-Korokoro (Study Area 2)

S/No	Plume Extent(m)	Coordinates		Label	Comment
		Easting	Northing		
1	80	312835	524370	AH1	Low-Impact
2	135	312934	524389	AH2	Low-Impact
3	35	312886	524393	AH3	Low-Impact
4	125	312762	524344	AH4	Low-Impact
5	115	312745	524312	AH5	Medium-Impact
6	105	312755	524319	AH6	Medium-Impact
7	80	312780	524290	AH7	High-Impact
8	NA	312896	524482	C	Control

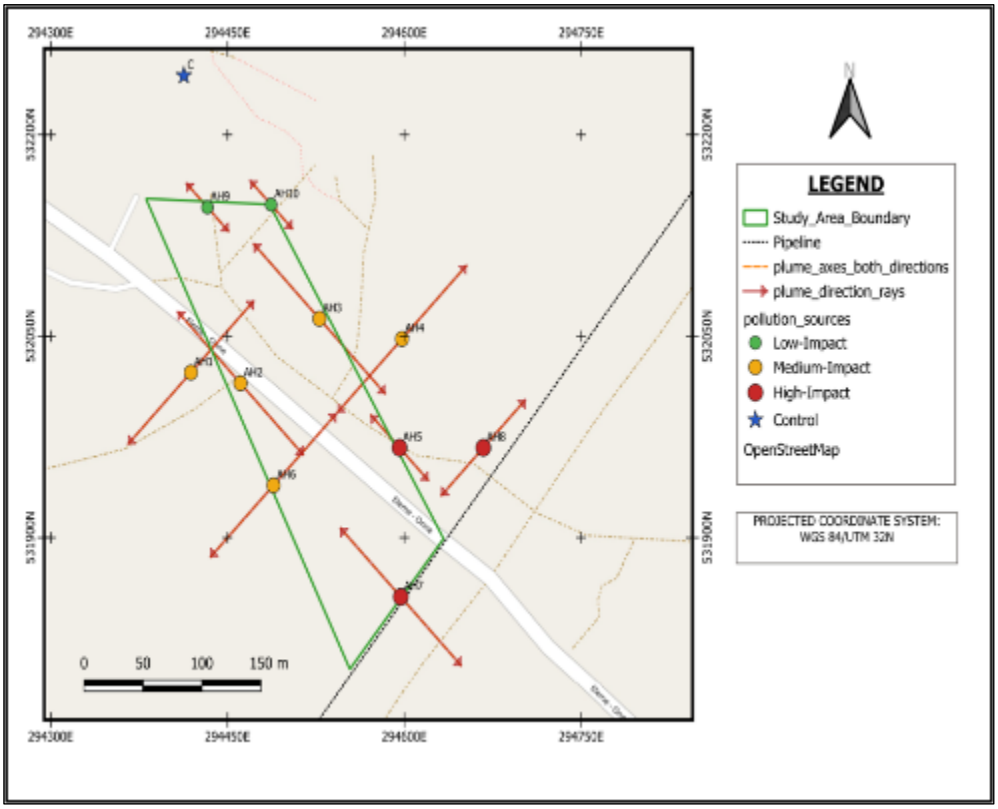


Figure 5: Spatial Distribution of Hydrocarbon Pollution Source (NPSC Pipeline), Auger-Hole Points, Crude Oil Impact Classifications, and Inferred Plume Migration within the Study Area (Area 1), Ajeokpori,Ogale

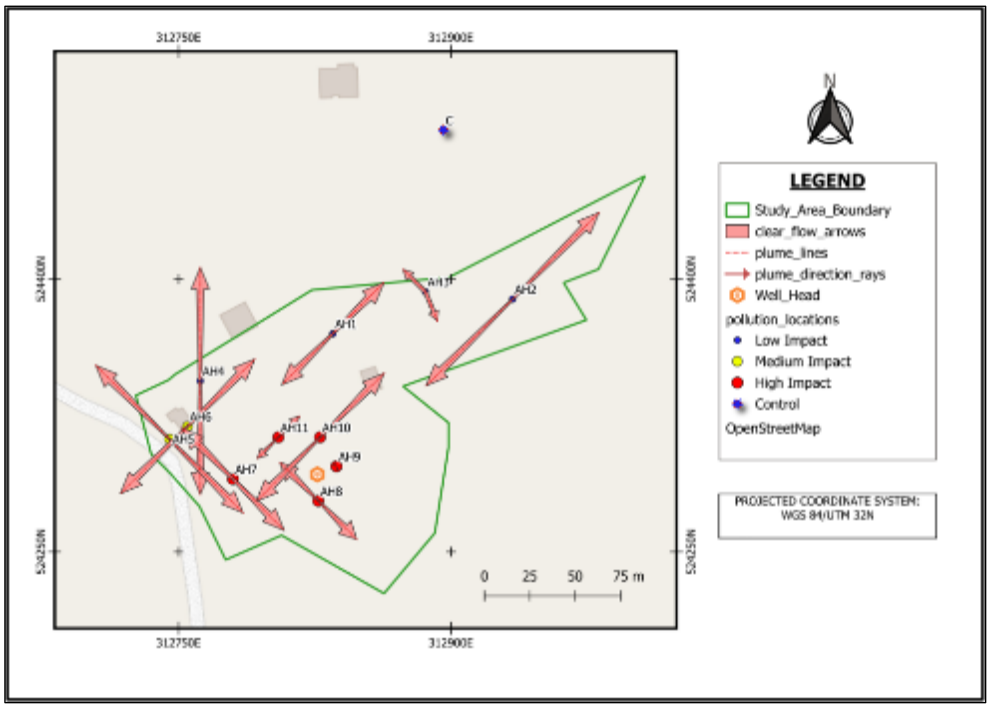


Figure 6: Spatial Distribution of Hydrocarbon Pollution Source (Well-Head 003), Auger-Hole Points, Crude Oil Impact Classifications, and Inferred Plume Migration within the Study Area (Area 2), Aabue-Korokoro

4.1 Data Analysis, Interpretation

Two-dimensional (2D) resistivity inversion tomograms were prepared for all the survey lines (tables 1 - 4). The tomograms were processed with two inversion software programs using different computer algorithms, such as the RES2DINV, based on the finite difference method, and EarthImager 2D, based on the finite element method. The tomograms obtained by the two software packages were very similar, regardless of the different processing algorithms used, (figures 7 and 8) which indicates the consistency and reliability of the inversion results. The results of all survey lines in the study area 1 (Ajeopkori) and study area 2 (Aabue-Korokoro) were computed with the RESD2DINV and EarthImager 2D through lines 1 – 7 in study area 1, and lines 1 – 7 in study area 2 accordingly

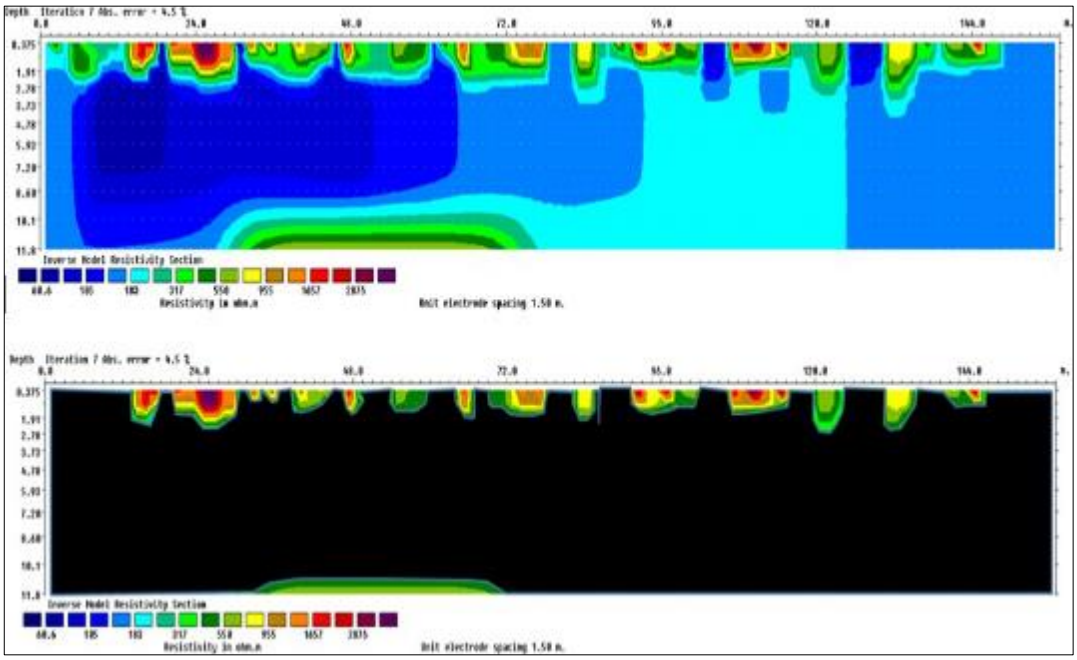


Figure 7: Processed electrical resistivity tomogram for Line 1 using RES2DINV software (dark area highlighted on second tomogram shows oil contaminated zones with resistivity values ≤600 Ωm)

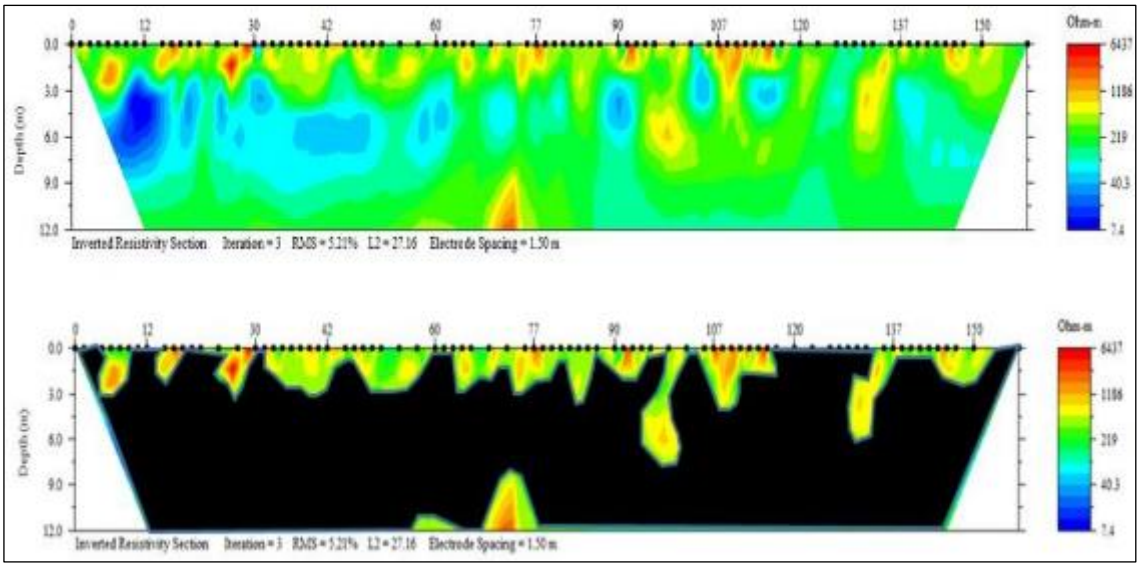


Figure 8: Processed electrical resistivity tomogram for Line 1 using Earth-Imager software (dark area highlighted on second tomogram shows oil contaminated zones with resistivity values ≤600 Ωhm)

5 RESULTS AND DISCUSSION

5.1 Ajeokpori, Study Area 1

The results show variation in the reported lateral extent and impact classification of hydrocarbon plumes at seven sampling locations (AH1–AH7), with an additional control location (C). Plume extents range from 68 m at AH5 to 157 m at AH3. Five locations—AH1, AH2, AH3, AH4, and AH6—are classified as medium-impact, while AH5 and AH7 are classified as high-impact.

The medium-impact locations have relatively similar plume extents, ranging from 150 to 157 m. AH1, AH2, and AH6 each record an extent of 150 m, while AH4 and AH3 record 154 and 157 m, respectively. This indicates broadly comparable lateral spread at these locations. However, similar plume lengths do not establish that the locations contain equal contaminant concentrations or volumes. Furthermore, where an interpreted plume extends across the entire surveyed profile, its reported length may represent the observed extent within the survey rather than its complete lateral boundary.

The high-impact locations demonstrate that plume extent and impact severity are distinct characteristics. AH5 has the shortest reported plume extent, at 68 m, whereas AH7 has an extent of 144 m. The coordinates indicate spatial separation between the impact categories. AH5 and AH7 have almost identical eastings (294596 and 294597) but differ in northing by 111 coordinate units. Assuming the coordinates belong to the same projected system expressed in metres, the two high-impact locations are approximately 111 m apart along a nearly north–south alignment. Both also lie south of AH1–AH4. This pattern identifies an area for closer investigation, but it does not establish a connected plume or its transport direction.

For the ERT investigation, these results provide a basis for selecting verification and monitoring locations. AH5 and AH7 warrant targeted assessment because of their high-impact classifications, while the medium-impact locations require sampling across the reported plume boundaries and depth intervals. Table 6 supports comparison of lateral extent and spatial distribution of the impacted points.

5.2 Aabue-Korokoro (Well 003) Study Area 2

The results indicate variation in the reported lateral extent and impact classification of hydrocarbon contamination across sampling locations AH1–AH7. Plume extents range from 35 m at AH3 to 135 m at AH2, with a mean of approximately 96.4 m. Four locations (AH1–AH4) are classified as low-impact, two (AH5 and AH6) as medium-impact, and one (AH7) as high-impact. This distribution suggests spatially uneven impact in the area.

The low-impact locations display considerable variation in plume extent. AH2 and AH4 have the longest reported extents, at 135 and 125 m, respectively, whereas AH1 records 80 m and AH3 records only 35 m. These results demonstrate that a low-impact classification does not necessarily correspond to a small lateral footprint. The relatively extensive plumes at AH2 and AH4 may represent broadly distributed contamination of lower intensity. The medium-impact locations, AH5 and AH6, have plume extents of 115 and 105 m, respectively. Their coordinates place them close together in the southwestern part of the area sampled. Assuming a common projected coordinate system expressed in metres, they are approximately 12.2 m apart. Their proximity and similar classifications identify a cluster demanding closer investigation.

AH7 is classified as high-impact and relatively concentrated hotspot despite having a plume extent of 80 m, equal to that of low-impact AH1 and shorter than those of both medium-impact locations. This comparison highlights the distinction between lateral extent and impact severity.

The coordinates reveal a spatial pattern in which the medium-impact locations occur southwest of AH1–AH3, while high-impact AH7 is the southernmost sampled location. This arrangement suggests that the southern and southwestern portions warrant targeted assessment.

The control point, C, lies north of all impacted sampling locations and provides a potential background comparison. The Background suitability was established through olfactive, laboratory analysis and comparable soil, depth, and hydrogeological conditions.

The results support targeted verification at AH7 and the AH5–AH6 cluster, alongside boundary sampling around the extensive low-impact interpretations at AH2 and AH4.

5.3 Major Findings

In Study Area 1, the high-impact location AH5 had the shortest extent (68 m), while medium-impact locations had the longest (150-157 m). Similarly in Study Area 2, high-impact AH7 (80 m) was shorter than low-impact AH2 (135 m).

- Study Area 1 (Ajeokpori) - Medium-Impact Dominance: 71.4% of locations (5 of 7) are medium-impact with comparable lateral spreads (150-157 m), indicating a broadly distributed contamination front along the NPSC pipeline corridor.
- Study Area 1 - Southern High-Impact Cluster: Two high-impact locations (AH5 and AH7) are spatially isolated ~111 m apart on the same easting (294596E / 294597E) and located south of the medium-impact group, defining a priority zone for immediate remediation.
- Study Area 2 (Aabue-Korokoro) - Low-Impact Dominance with Southwest Migration: 57% of locations are low-impact but with highly variable extents (35-135 m), suggesting diffuse low-intensity contamination.
- Study Area 2 - Southwest Hotspot Cluster: Medium-impact AH5 and AH6 are clustered at ~12.2 m separation in the southwestern sector, with high-impact AH7 as the southernmost point, indicating a southward increase in impact severity.

Control Validation: The control point (C) in both areas, located north of impacted zones and validated by olfactive, laboratory, and hydrogeological criteria, confirms anthropogenic hydrocarbon input at impacted locations.

6 CONCLUSION

This study carried out geospatial distribution and mapping of hydrocarbon-contaminated sites in Ajeokpori (Study Area 1) and Aabue-Korokoro Well 003 (Study Area 2) in the Niger Delta, Nigeria. The integration of georeferenced auger hole locations, empirical hydrocarbon impact classification based on TPH, and lateral plume extent from ERT interpretation revealed spatially heterogeneous contamination. In Ajeokpori (Study Area 1), five of seven locations (AH1, AH2, AH3, AH4, AH6) were classified as medium-impact with lateral extents between 150 and 157 m, while two locations (AH5 with 68 m and AH7 with 144 m) were high-impact. In Aabue-Korokoro (Study Area 2), four locations (AH1–AH4) were low-impact (35–135 m), two (AH5–115 m, AH6–105 m) medium-impact, and one (AH7–80 m) high-impact, with a mean plume extent of 96.4 m. The study established that lateral plume extent and impact severity are distinct parameters. High-impact classification does not necessarily correspond to larger lateral footprint, as demonstrated by AH5 in Study Area 1 and AH7 in Study Area 2. Spatial analysis identified distinct clusters of concern: a north-south aligned high-impact cluster (AH5–AH7, ~111 m apart) south of the main pipeline corridor in Study Area 1, and a southwestern medium-impact cluster (AH5–AH6, ~12.2 m apart) with a southernmost high-impact hotspot (AH7) in Study Area 2. This pattern indicates a potential southward and southwestward migration of contaminants requiring focused attention. The georeferenced framework developed provides a verifiable baseline for remediation planning and ERT validation.

Recommendation

The study recommends the following measures to improve the sites environmental conditions of the studied areas. Targeted remediation should prioritize high-impact locations AH5 and AH7 in Study Area 1 and AH7 in Study Area 2, as well as the medium-impact cluster AH5–AH6 in Study Area 2. To establish effective boundary delineation, additional sampling should be conducted beyond the reported plume limits (150–157 m in Study Area 1 and 125–135 m in Study Area 2), as plumes extending across entire ERT profiles likely exceed observed extents. ERT Verification: ERT surveys should be focused on the identified southern and southwestern clusters to delineate vertical extent, depth of free-phase product, and groundwater interaction. Continuous Groundwater Monitoring (CGM): Installation of groundwater monitoring wells south and southwest of the high-impact clusters is recommended to assess potential leaching and off-site migration. Regulatory Compliance: All impacted soils exceeding the DPR/EGASPIN intervention value of 5,000 mg/kg (high-impact) and target value of 50 mg/kg (low and medium-impact) should be subjected to approved remediation technologies.

STATEMENTS ON COMPLIANCE WITH ETHICAL STANDARDS

Acknowledgments

We thank all the staff members of the Hydrocarbon Pollution Remediation Project (HYPREP), and the Department of Geology, Rivers State University for providing working facilities and their encouragement.

Funding Source

This research was supported by the Hydrocarbon Pollution Remediation Project (HYPREP), Federal Ministry of Environment, Nigeria. _ HYP /ADM/121/170

Disclosure of conflict of interest

The authors declare no conflicts of interest regarding this manuscript.

Contribution to Knowledge

The study demonstrates the importance of dissociating lateral extent from impact classification in hydrocarbon assessment and provides a geospatial model for prioritizing remediation in Niger Delta communities using integrated GPS and ERT data.

REFERENCES

[1] United Nations Environment Programme. Environmental assessment of Ogoniland. Nairobi: United Nations Environment Programme; 2011.

[2] Nwilo PC, Badejo OT. Oil spill problems and management in the Niger Delta. International Oil Spill Conference Proceedings. 2005;2005(1):567-570.

[3] Benjamin JI, Okeke FI. Geospatial analysis of oil spill in the selected parts of the Niger Delta. Journal of Environmental and Geographical Studies. 2023;2(1):121-135. doi:10.58425/jegs.v2i1.121.NOSDRA. (2023). Nigerian oil spill monitor: Cumulative spill data 2006-2023. National Oil Spill Detection and Response Agency.

[4] National Oil Spill Detection and Response Agency. Nigerian oil spill monitor: cumulative spill data 2006-2023. Nigeria: National Oil Spill Detection and Response Agency; 2023.

[5] Ahmed NO, Obafemi AA, Udom GJ. Geospatial variability and distribution of total petroleum hydrocarbons (TPH) in soot-contaminated rain and rivers at Oyigbo, Niger Delta, Nigeria. Journal of Geography, Environment and Earth Science International. 2024;28(3):1-30. doi:10.9734/jgeesi/2024/v28i3753.

[6] Balde A, Akpotu E, Liu F, Momeni M. Geo-spatial analysis of oil spill distribution and susceptibility in the Niger Delta region of Nigeria. Journal of Geographic Information System. 2018;10(5):438-455.

[7] Onomhoale NA, Yunusa LJ, Senbore S, Apata MD, Ojogbo P, Itiveh ES. Hydrochemical dispersion and geospatial correlation for source identification, transport, and fate of aerial petro-pollutants in the Niger Delta, Nigeria. Journal of Geoscience and Environment Protection. 2024;13(4):45-68.

[8] World Health Organization. Guidelines for drinking-water quality. 4th ed. Geneva: World Health Organization; 2017.

[9] Adejuwon JO. Climate change and coastal cities: the case of Lagos, Nigeria. Journal of Environmental Studies. 2012;21(1):1-11.

[10] Udoh FE. Climate variability and water resources in the Niger Delta, Nigeria. Journal of Water Resources and Environmental Engineering. 2016;8(1):1-11.

[11] Nwafor JC. Environmental impact assessment of the Niger Delta oil spills. Journal of Environmental Management. 2006;78(2):123-134.Akpokodje, E. G. (2010). The Niger Delta environment. In K. M. Bartholomew (Ed.), Environmental issues and management in the Niger Delta (pp. 35–52). Port Harcourt: Paragraphics.

[12] Nwankwoala HO, Amadi AN. Geology and hydrogeology of the Niger Delta. International Journal of Geology, Earth and Environmental Sciences. 2013;3(1):28-37.

[13] Akpokodje EG. The Niger Delta environment. In: Bartholomew KM, editor. Environmental issues and management in the Niger Delta. Port Harcourt: Paragraphics; 2010. p. 35-52.

[14] Short KC, Stäuble AJ. Outline of geology of Niger Delta. AAPG Bulletin. 1967;51(5):761-779. doi:10.1306/5D25C0CF-16C1-11D7-8645000102C1865D.

[15] Reijers TJA. Stratigraphy and sedimentology of the Niger Delta. Geologos. 2011;17(3):133-162.

[16] Doust H, Omatsola E. Niger Delta. In: Edwards JD, Santogrossi PA, editors. Divergent/passive margin basins. Tulsa (OK): American Association of Petroleum Geologists; 1990. p. 201-238.

[17] Oyinkuro OA, Wariebi KA. Hydrocarbon spill site characterization by electrical resistivity tomography and ground penetrating radar methods: a review. Asian Journal of Environment & Ecology. 2017;4(3):1-9.

[18] Advanced Geosciences, Inc. EarthImager 2D and 3D resistivity and induced polarization inversion software user guide. Austin (TX): Advanced Geosciences, Inc.; 2014.

[19] Loke MH. Tutorial: 2-D and 3-D electrical imaging surveys. Penang (Malaysia): Geotomo Software; 2018.

[20] Schwarzbach C, Börner RU, Spitzer K. Three-dimensional adaptive higher order finite element simulation for geo-electromagnetics: a parallel solution approach. Geophysical Journal International. 2005;162(3):641-655.

[21] Loke MH. Electrical imaging surveys for environmental and engineering studies: a practical guide to 2-D and 3-D surveys. Geotomo Software; 2000.

[22] Loke MH, Barker RD. Rapid least-squares inversion of apparent resistivity pseudosections by a quasi-Newton method. Geophysical Prospecting. 1996;44(1):131-152. doi:10.1111/j.1365-2478.1996.tb00142.x.

[23] Sasaki Y. Resolution of resistivity tomography inferred from numerical simulation. Geophysical Prospecting. 1992;40(4):453-463. doi:10.1111/j.1365-2478. 1992.tb00536.x.

[24] Loke MH, Dahlin T. A comparison of the Gauss-Newton and quasi-Newton methods in resistivity imaging inversion. Journal of Applied Geophysics. 2002;49(3):149-162. doi:10.1016/S0926-9851(01)00106-9.